

# Orientation-Dependent Plasticity in Metal Nanowires under Torsion: Twist Boundary Formation and Eshelby Twist

Christopher R. Weinberger,<sup>\*,†</sup> and Wei Cai<sup>\*</sup>

Department of Mechanical Engineering, Stanford University, Stanford, California 94305

**ABSTRACT** We show that the plastic deformation of nanowires under torsion can be either homogeneous or heterogeneous, regardless of size, depending on the wire orientation. Homogeneous deformation occurs when  $\langle 110 \rangle$ -oriented face-centered-cubic metal wires are twisted, leading to the nucleation of coaxial dislocations, analogous to the Eshelby twist mechanism. Heterogeneous deformation is predicted for  $\langle 111 \rangle$  and  $\langle 100 \rangle$  wires under torsion, localized at the twist boundaries. These simulations also reveal the detailed mechanisms of twist boundary formation from dislocation reactions.

**KEYWORDS** Nanowires, mechanical properties, dislocations, plasticity

The strength and plasticity of metals at the micrometer scale and below have been of great interest as they relate to the reliability and manufacturability of small-scale devices. Strength has been shown to dramatically increase as the diameters of metallic micropillars drop below  $10 \mu\text{m}$ .<sup>1</sup> Plasticity at smaller length scales also appears to be more heterogeneous, characterized by localized strain bursts in the sample.<sup>2,3</sup> As a result, difficulties are expected in metal forming at the micrometer scale,<sup>3</sup> such as bending or twisting of metallic microwires. Twisting experiments of polycrystalline metal wires have also shown a dramatic increase of strength with decreasing diameter, in agreement with strain gradient plasticity theory.<sup>4</sup> However, many of the materials are single crystals at these scales. Given the tremendous interest in the compressive and tensile tests on single crystal micropillars, surprisingly little is known about the plastic response of single crystal microwires in torsion.

In wires under torsion, it is natural to expect heterogeneous plastic deformation by the formation of twist boundaries, which are planar networks of screw dislocations perpendicular to the applied torque.<sup>5,6</sup> The other possible dislocation mechanism that can relieve torque is a screw dislocation parallel to the applied torque.<sup>7</sup> Eshelby<sup>8</sup> originally considered these types of dislocations as grown-in defects in whiskers, and this has recently been observed in the formation of chirally branched nanowires.<sup>9,10</sup> However, the conditions under which coaxial dislocations form as a deformation mechanism largely remain unknown. The consequence of this mechanism on the mechanical behavior of

wires under torsion has not received much attention, since the formation of twist boundaries generally requires less energy.

In this work, we investigate the plastic response of pristine single crystal nanowires in torsion using molecular dynamics (MD) simulations. We find that the wire orientation determines whether twist boundaries form as dislocation networks or coaxial dislocations nucleate. This is in contrast to uniaxial loading, in which dislocations gliding across slip planes inclined to the wire axis are always the deformation mechanism regardless of wire orientation. Furthermore, when coaxial dislocations nucleate, the plastic deformation is remarkably homogeneous, both along the wire and in its cross section. This means plasticity at the submicrometer scale is not necessarily heterogeneous and the aforementioned difficulty in metal forming at this scale may be avoided for certain deformation modes.

Nanowires with three orientations,  $\langle 110 \rangle$ ,  $\langle 111 \rangle$ , and  $\langle 100 \rangle$ , are considered. Torsion periodic boundary conditions<sup>11</sup> are used in molecular dynamics (MD) simulations to eliminate end effects that occur when artificial grips are used. This boundary condition is similar to a standard periodic boundary condition along the length of the wire except that the periodic images are rotated relative to each other. Two face-centered-cubic (fcc) metals, gold and aluminum, are studied to ensure generality of the results and to determine the effects of the stacking fault energy. We twist three different diameters for both materials: 5, 7.5, and 10 nm. Since the interatomic potential for Au<sup>12</sup> has a stacking fault energy of  $31 \text{ mJ/m}^2$ , which is about 5 times less than the Al potential<sup>13</sup> of  $146 \text{ mJ/m}^2$ , we also look at 15 and 20 nm diameter Au nanowires. The wires are twisted in each simulation at a constant rate resulting in a nominal engineering surface strain rate of  $4 \times 10^8 \text{ s}^{-1}$ . This is done by applying an incremental twist per unit length every 5000

\* To whom correspondence should be addressed, crweinb@sandia.gov and caiwei@stanford.edu.

† Current address: Sandia National Laboratories, P.O. Box 5800, MS 1411, Albuquerque, NM 87125-1411.

Received for review: 09/14/2009

Published on Web: 12/23/2009



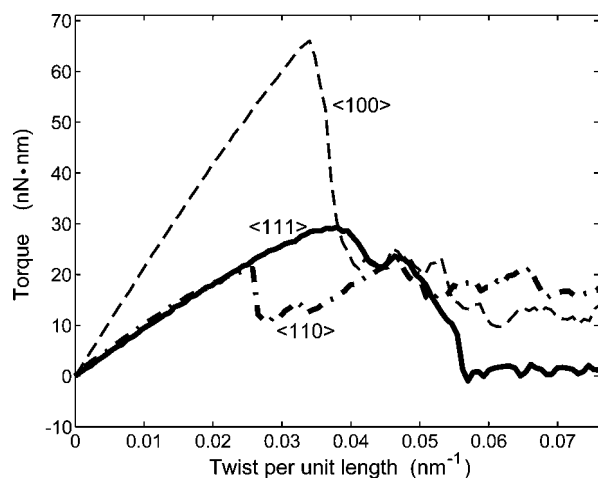


FIGURE 1. Torque twist curves for the 5 nm diameter Au nanowires with three different orientations.

time steps with a time step of 1 fs. For convenience, we define an engineering shear strain rate as  $\dot{\gamma} = \beta r$ , where  $\beta$  is the twist rate per unit length and  $r$  is the radius where the strain is evaluated. For better comparison between simulations with different diameters, the twist rate per unit length  $\beta$  was adjusted so that the surface strain rate is a constant. During the torsion simulations, the box length along the wire axis is allowed to adjust its length in response to the instantaneous virial stress to remove the axial stress.<sup>14</sup>

Each simulation starts with a pristine, defect-free nanowire. The applied twist provides the sole driving force for defect nucleation, which occurs naturally through the individual interactions of the atoms. Dislocation nucleation initiates yield in each wire, which is observed in Figure 1. The plasticity in these simulations is dominated by dislocation nucleation; however dislocation patterning still occurs by the organization of the dislocations after nucleation.

Figure 1 plots representative torque–twist curves for 5 nm diameter gold nanowires, one for each orientation.  $\langle 110 \rangle$ -oriented wires yield by the nucleation of coaxial dislocations as shown in Figure 2. In fcc metals, we expect dislocations to nucleate on  $\{111\}$  planes with maximum resolved shear stress. According to linear elasticity, the planes of maximum shear stress for circular sections in torsion are planes perpendicular to the wire axis and planes containing the wire axis, as indicated in Figure 2a. For  $\langle 110 \rangle$ -oriented wires, there are two  $\{111\}$  planes that intersect the wire axis, making an angle of  $71^\circ$  to each other. These are indeed the planes on which dislocations are first nucleated, as easily seen in Figure 2b. The dislocations that nucleate are either perfect screw dislocations or the leading partial of a perfect screw dislocation since the screw components directly relieve the applied torque.

The deformation mechanism for  $\langle 110 \rangle$  wires is essentially the Eshelby twist mechanism<sup>8</sup> in reverse. While Eshelby predicted that grown-in coaxial screw dislocations causes the wire to twist on its own, our results show that coaxial

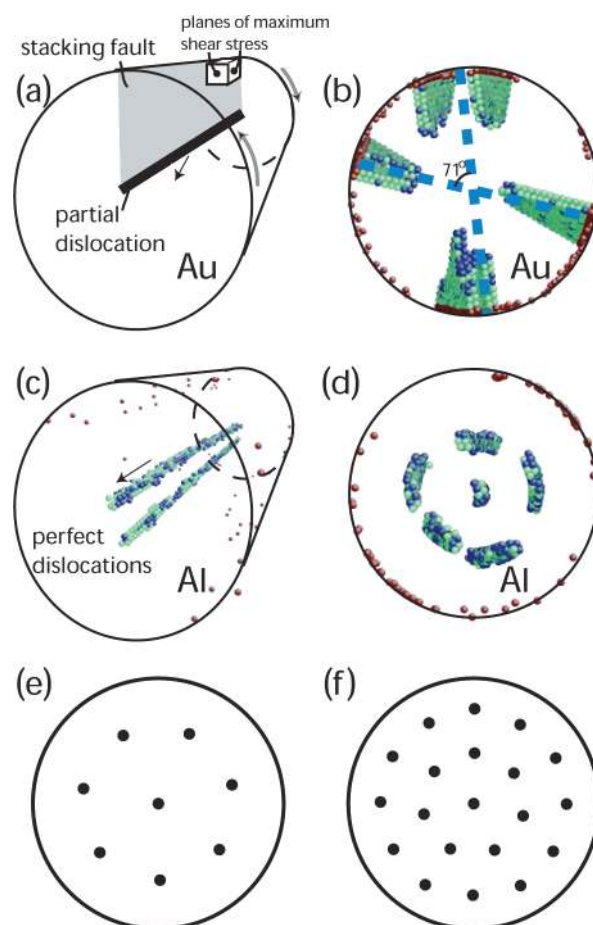


FIGURE 2. Plasticity as observed in  $\langle 110 \rangle$ -oriented 10 nm diameter nanowires. (a) Schematics showing stacking fault area bounded by a partial dislocation. The straight arrow indicates the Burgers vector. The curved arrows indicate the direction of twist. A stress cube is drawn to indicate the planes of maximum shear stress. (b) End view of the Au nanowire. Only atoms with a centrosymmetry parameter<sup>15</sup> significantly different from zero are plotted, showing the partial dislocations and the stacking fault area. (c) 3D view of perfect dislocations nucleated in Al nanowire. (d) End view of Al nanowire containing six perfect dislocations along its axis. (e) Equilibrium distribution of eight screw dislocations in an elastic cylinder predicted by a two-dimensional dislocation dynamics model. (f) Equilibrium distribution of 20 screw dislocations in the cylinder.

dislocations can also nucleate when a defect-free wire is twisted by an external load. The screw dislocations extend through the entire length of the wire and are distributed quite uniformly in the wire cross section, making the deformation surprisingly homogeneous even at such a small scale.

For 10 nm diameter wires, we observe partial dislocation nucleation in Au (Figure 2b) and both perfect and partial dislocation nucleation in Al (parts c and d in Figure 2). However, both perfect and partial dislocations are observed in 20 nm diameter Au wires, suggesting that this is a size effect instead of a fundamental difference between the two metals. We expect the fraction of perfect dislocations in a Au wire to increase as the wire radius further increases.

The difference between partial and perfect dislocations has an important consequence for the stability of the

dislocations inside the wire and affects the reversibility of the deformation. When a moderately twisted  $\langle 110 \rangle$  5 nm diameter gold nanowire is unloaded to zero torque (not shown here), the partial dislocations that have nucleated escape to the surface, reversing a large fraction of the inelastic deformation. The stacking fault connecting the partial dislocations and the wire surface helps pull the dislocations out. For a sufficiently thin wire subjected to moderate twist, all dislocations escape upon unloading, making the deformation completely reversible. The complete reversibility of torsional deformation of  $\langle 110 \rangle$  wires may find applications in some nanoelectrical mechanical system (NEMS) devices.

However, if perfect dislocations were nucleated, these dislocations stay inside the wire even when the applied torque is zero. This confirms that multiple screw dislocations can be stable in a torque-free wire.<sup>10</sup> To test whether a large number of perfect screw dislocations can be metastable within the wire, we performed two-dimensional dislocation dynamics (DD) simulations in an elastic cylinder subjected to zero torque. A two-dimensional dislocation dynamics (DD) code is developed to simulate the behavior of screw dislocations in  $\langle 110 \rangle$  oriented wires. The wire is modeled as an elastically isotropic cylindrical rod. The forces on the dislocations are computed by superimposing the fields of infinitely long screw dislocations in cylinders derived by Eshelby.<sup>8,16</sup> The total force on a dislocation is the sum of several contributions, including the Peach–Koehler force from other dislocations in an infinite medium, image force required to make the cylindrical surface traction free, and image torque forces required to make the rod torque free. The initial positions of the dislocation are randomly chosen within the cylinder. The dislocations are allowed to relax in the direction of the total Peach–Koehler forces, until the forces on all dislocations are zero.

We find that in general the dislocations reach an equilibrium configuration easily without escaping the cylinder. Furthermore, their equilibrium distribution is remarkably uniform, as shown in parts e and f of Figure 2, consistent with the MD predictions. Given the size effect on the preference of partial or perfect dislocations, we expect reversibility of torsional deformation only in wires of sufficiently small diameter.

Contrary to  $\langle 110 \rangle$  wires,  $\langle 111 \rangle$  wires deform heterogeneously through the formation of twist boundaries. All dislocations nucleate on a few  $\{111\}$  atomic planes that are adjacent to each other, which are also the planes of maximum shear stress. For the first time, our simulations reveal the full mechanistic detail of the  $\{111\}$  twist boundary formation from dislocation reactions, which is shown in Figure 3.

Initially, two partial dislocations nucleate on the  $\{111\}$  plane as shown in Figure 3a. In Figure 3b, the trailing partials have nucleated and the resulting two perfect dislocations have formed a junction of a “Y” shape. This is a junction of three screw dislocations, each having one of the three

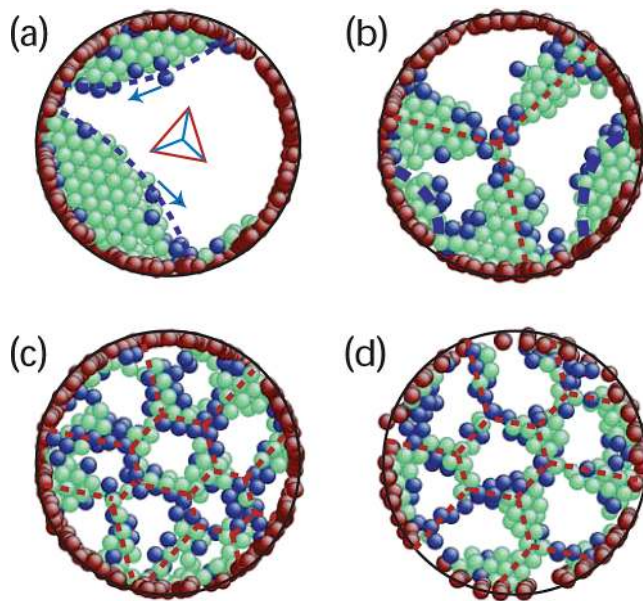


**FIGURE 3.** Plasticity as observed in  $\langle 111 \rangle$  oriented 5 nm diameter Au nanowires. (a) Two partial dislocation nucleate. The arrows indicate their Burgers vector. The triangle marks the three perfect Burgers vectors on this plane. The lines inside the triangle mark the three partial Burgers vectors on this plane. (b) Two perfect dislocations react to form a screw “Y” junction. (c) The evolution to a hexagonal array. (d) A similar hexagonal array during untwisting.

perfect Burgers vectors available on the  $\{111\}$  plane. This junction is stable under the applied torque and is the embryo of the twist boundary. It is the smallest dislocation network with only one internal node. When another perfect dislocation is nucleated from the surface, one of the three arms readily reacts with it to form another junction and the number of internal nodes of the dislocation network grows by one. The process of dislocation nucleation and junction formation repeats itself, leading to the formation of a hexagonal dislocation network shown in Figure 3c.

As the twisting continues, traces of individual dislocations are eventually lost in the (high-angle) twist boundary. But the same hexagonal network becomes visible again when the wire is untwisted, Figure 3d. The dislocation network is gradually dismantled when the wire is twisted in the opposite direction. The final structure before complete destruction of the network is again a “Y” junction, just like that shown in Figure 3b. Our results show that the  $\{111\}$  twist boundary evolves easily from the embryonic structure (without dislocation pile-up). This is different from the pathway hypothesized earlier,<sup>6</sup> which required continued dislocation nucleation between piled-up dislocations to maintain the growth of the twist-boundary.

Twisting a  $\langle 100 \rangle$  wire also leads to the formation of a twist boundary perpendicular to the wire axis. The resulting dislocation network is compact along the wire, and the deformation is very heterogeneous. However, the formation mechanism of the  $\langle 100 \rangle$  twist boundary is different from that of  $\langle 111 \rangle$ . This is because several  $\{111\}$  slip planes experi-



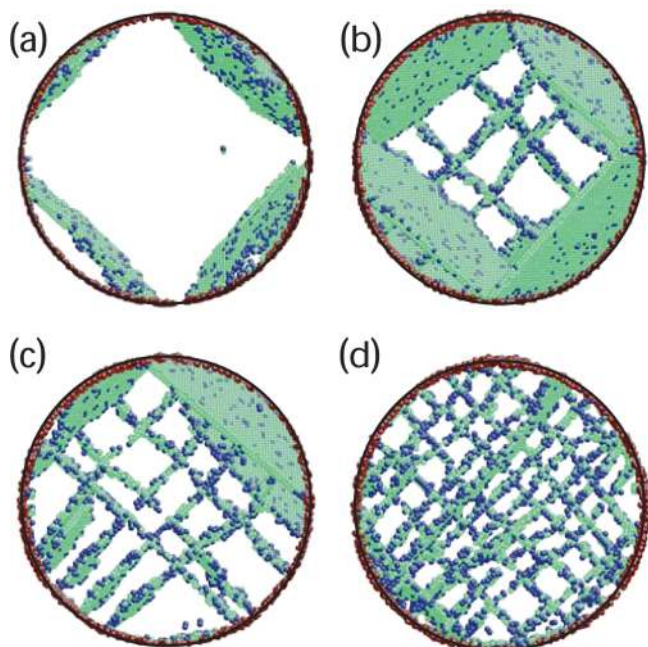


**FIGURE 4.** Plasticity as observed in  $\langle 100 \rangle$  oriented 20 nm diameter Au nanowires. Dislocations nucleate from the surface and organize into a rectangular array of screw dislocations.

ence the same magnitude of shear stress and they are all at an angle to the twist boundary that forms. Because dislocations from several slip systems are equally likely to nucleate, this formation process is expected to be representative of what might happen when a wire with a pre-existing dislocation network is twisted.

Figure 4 shows the nucleation of dislocations in a 20 nm diameter Au nanowire and arrangement into a  $\{100\}$  twist boundary. Wide stacking fault areas are observed when the leading partials alone are nucleated. After the trailing partials nucleate, the perfect dislocations reorient themselves to be screw dislocations perpendicular to the wire axis. Once the first two perpendicular dislocations meet at a plane, the rest of the dislocations also aggregate on the same plane. The result is a rectangular network of screw dislocations forming a  $\{100\}$  low angle twist boundary.

While it may be challenging to test the homogeneity of plastic deformation of  $\langle 110 \rangle$  wires directly by electron microscopy, it will be useful to perform experiments to test the other predictions of the MD simulations. First, when the deformation is homogeneous (for  $\langle 110 \rangle$  wires) the load drop upon yield is much smaller than that when the deformation is heterogeneous (for  $\langle 111 \rangle$  and  $\langle 100 \rangle$  wires). The simulations also predict that the torsional strength of the  $\langle 100 \rangle$  twist boundary is much higher than that of the  $\langle 111 \rangle$  twist boundary, which can be tested experimentally. These predictions are not limited to nanowires as they are not size

dependent and should hold for dislocation free whiskers or microwires.

In summary, we have presented the orientation-dependent plasticity and yield in single crystal metallic nanowires in torsion. Plasticity occurs by nucleation of dislocations from the surfaces which organize under the influence of the strain gradient. Wires oriented along  $\langle 110 \rangle$  yield through the nucleation of coaxial dislocations which causes the plasticity to be homogeneous. The wires also retain a significant fraction of their strength after yield. In the  $\langle 111 \rangle$  and  $\langle 100 \rangle$  orientations the wires yield through the formation of twist boundaries perpendicular to the wire axis and the resulting plastic deformation is heterogeneous. This orientation dependence is controlled by the availability of slip planes on which dislocations can easily nucleate. This effect is found to be robust, even though the detailed dislocation structure formed in each simulation is not unique, given the random nature of nucleation. In addition, since plasticity is not necessarily heterogeneous but depends on wire orientation, this suggests that fabrication of nanoscale metallic components may not be as difficult as previously thought. We also expect that testing these predictions by twisting pristine metal nanowires or whiskers will provide new insight on the fundamental deformation mechanisms of materials.

**Acknowledgment.** The work is supported by National Science Foundation Career Grant CMS-0547681, Air Force office of Scientific Research/Young Investigator Program grant, the Army High Performance Computing Research Center at Stanford, and a Benchmark Stanford Graduate Fellowship (to C.R.W.).

## REFERENCES AND NOTES

- Uchic, M.; Dimiduk, D.; Florando, J.; Nix, W. *Science* **2004**, *305*, 986.
- Brinckmann, S.; Kim, J.-Y.; Greer, J. R. *Phys. Rev. Lett.* **2008**, *100*, 155502.
- Csikor, F. F.; Motz, C.; Weygand, D.; Zaiser, M.; Zapperi, S. *Science* **2007**, *318*, 251.
- Fleck, N. A.; Muller, G. M.; Ashby, M. F.; Hutchinson, J. W. *Acta Metall. Mater.* **1994**, *42*, 475.
- Packeiser, D.; Gwinner, D. *Philos. Mag.* **1980**, *42*, 661.
- McClintock, F. A.; Prinz, F. *Acta Metall.* **1983**, *31*, 827.
- Gao, H.; Huang, Y.; Nix, W. D.; Hutchinson, J. W. *J. Mech. Phys. Solids* **1999**, *47*, 1239.
- Eshelby, J. D. *J. Appl. Phys.* **1953**, *24*, 176.
- Bierman, M. J.; Lau, Y. K.; Kvit, A. V.; Schmitt, A. L.; Jin, S. *Science* **2008**, *320*, 1060.
- Zhu, J.; Peng, H.; Marshall, A. F.; Barnett, D. M.; Nix, W. D.; Cui, Y. *Nat. Nanotechnol.* **2008**, *3*, 477.
- Cai, W.; Fong, W.; Elsen, E.; Weinberger, C. R. *J. Mech. Phys. Solids* **2008**, *56*, 3242.
- Park, H. S.; Zimmerman, J. A. *Phys. Rev. B* **2005**, *72*, No. 054106.
- Mishin, Y.; Farkas, D.; Mehl, M. J.; Papaconstantopoulos, D. A. *Phys. Rev. B* **1999**, *59*, 3393.
- Parrinello, M.; Rahman, A. *J. Appl. Phys.* **1981**, *52*, 7182.
- Kelchner, C. L.; Plimpton, S. J.; Hamilton, J. C. *Phys. Rev. B* **1998**, *58*, 11085.
- Eshelby, J. D. Boundary Problems. In *Dislocations in Solids*; North Holland Publishers: Amsterdam, 1979; Vol. 1, p 167.